



Effect of iron content on selectivity in isomerization of α -pinene oxide to campholenic aldehyde over Fe-MMM-2 and Fe-VSB-5

M.N. Timofeeva^{a,b,*}, V.N. Panchenko^a, Zubair Hasan^c, Nazmul Abedin Khan^c, M.S. Mel'gunov^a, A.A. Abel^a, M.M. Matrosova^a, K.P. Volcho^d, Sung Hwa Jhung^{c,1}

^a Boreskov Institute of Catalysis SB RAS, Prospekt Akad. Lavrentieva 5, 630090 Novosibirsk, Russian Federation

^b Novosibirsk State Technical University, Prospekt K. Markska 20, 630092 Novosibirsk, Russian Federation

^c Department of Chemistry and Green-Nano Materials Research Center, Kyungpook National University, Sankyuck-Dong, Buk-Ku, Daegu 702-701, Republic of Korea

^d Novosibirsk Institute of Organic Chemistry SB RAS, Prospekt Akad. Lavrentieva 9, 630090 Novosibirsk, Russian Federation



ARTICLE INFO

Article history:

Received 12 July 2013

Received in revised form 7 October 2013

Accepted 8 October 2013

Available online 17 October 2013

Keywords:

Isomerization of α -pinene oxide

Fe-VSB-5

Fe-containing mesoporous materials

Lewis acidity

ABSTRACT

Isomerization of α -pinene oxide to campholenic aldehyde (CA) was investigated over Fe-containing mesoporous mesophase materials (Fe-MMM-2) and microporous nickel phosphate molecular sieves (Fe-VSB-5). Activity and selectivity of reaction towards CA over Fe-containing materials was found to depend on iron content in materials that affects oligomeric state of Fe and amount of Lewis acid sites. In the presence of Fe-VSB-5 selectivity towards CA increased with increase in iron content in structure, while that decreased in the presence of Fe-MMM-2. This phenomenon is related to change in agglomeration of iron species in Fe-MMM-2 structure. The high selectivity towards CA in the presence of Fe-VSB-5 was suggested to arise from unique structure of these materials, which favours shape selectivity.

© 2013 Elsevier B.V. All rights reserved.

1. Introduction

Nowadays, considerable attention is focused on the development of new solid Lewis catalysts, which can be applied not only for works with fundamental scientific interest, but also for many applications at industrial level [1,2]. The main goal of the design of solid Lewis acids is the substitution of the traditional homogeneous acid catalysts, such as $ZnCl_2$, $AlCl_3$, $FeCl_3$ etc. [2,3] for solving all the well-known problems of the homogeneous acids. Zeolites and zeotype materials containing transition metal ions are the promising systems for catalysis. These materials are widely used as catalysts in alkylation and acylation of aromatic compounds [4–6], processes of isomerization and cyclization of terpenes [7–9].

Isomerization of terpene oxides is one of the important reactions for synthesis of intermediates for production of drugs, vitamins and fragrances. α -Pinene oxide (PO) is one of the key examples, which isomerizes rapidly in the presence of acids, thereby forming many products (Scheme 1). Trans-carveol (*trans*-carv) and campholenic aldehyde (CA) are industrially the most desired products

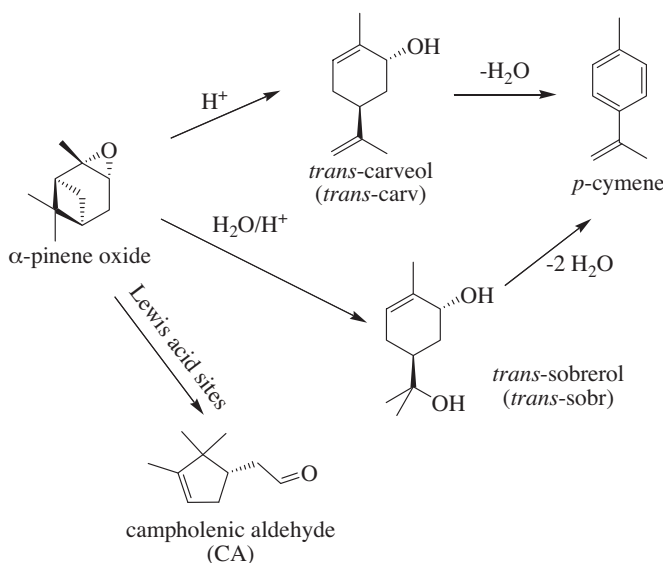
of PO isomerization, because they are highly valuable ingredients for the production of flavors. It is well-known that Lewis acid sites (LAS) favour the formation of CA, while Brønsted acid sites (BAS) lead to the formation of *trans*-carv, *trans*-sobrerol (*trans*-sobr) and *p*-cymene [3,10,11]. Note that the main attention in literatures is focused on synthesis of CA which is used in the fragrance industry for its sandalwood scent. $ZnCl_2$ and $ZnBr_2$ in benzene are the most active homogeneous systems with 85% selectivity towards CA [3]. However, the application of $ZnCl_2$ or $ZnBr_2$ has several disadvantages, such as lack of regeneration, corrosion problems, toxicity and wastewater pollution.

Many research groups try to find a truly heterogeneous catalyst system. Unfortunately, offered systems have not been competitive with the homogeneous system. However, several heterogeneous systems based on zeolites with good activities have been reported [10,12,13]. Thus, Hölderich et al. [10] found that the three-dimensional large pore system (7.4 Å) with supercages of 12 Å and large amount of mesopores make US-Y zeolites very suitable for isomerization of PO. Dealuminated of H-US-Y zeolite by HCl allows to obtain CA with a good yield. The selectivity towards CA was about 70% at 25 °C, but it could be improved to 80%, when reaction was carried out at -30 °C. It was suggested that the active sites are highly dispersed Lewis acid species (extra-framework aluminium) located within the zeolitic framework. Moreover, it was demonstrated that the performance of H-US-Y depends on the bulk

* Corresponding author. Tel.: +7 383 330 7284; fax: +7 383 330 8056.

E-mail addresses: timofeeva@catalysis.ru, [\(M.N. Timofeeva\)](mailto:mariya-timofeeva@yandex.ru), [\(S.H. Jhung\)](mailto:sung@knu.ac.kr).

¹ Tel: +82 53 950 5341; fax: +82 53 950 6330.



Scheme 1. Products obtained in the course of α -pinene oxide rearrangement.

Si₂/Al₂O₃ ratio. Yield of CA increases with decreasing aluminum content.

van Bekkum et al. [8] also demonstrated that Ti-BEA zeolite allows to obtain CA with high selectivity in both the liquid and vapour phases. The high activity was attributed to the presence of isolated, well-dispersed titanium sites in zeolite. Furthermore, it was suggested that structure of the zeolite with pore size comparable with size of reagents and intermediates may improve selectivity towards CA by shape-selectivity.

Ravindra et al. [7] investigated isomerization of PO over Al-MSU-S_{FAU} (Si/Al 70), which was synthesized from nanoclustered zeolite Y seeds as framework precursors. According to this synthesis, Al-MSU-S_{FAU} possesses a mesoporous structure with the walls having microporosity. The selectivity towards CA was 86% at 54% conversion of PO. It was suggested that reaction can occur within microporous channels. However, due to the short length of channels, reaction products can diffuse away from the active site before further reaction to other isomers occurs.

Fellenz et al. [14] demonstrated that the selectivity towards CA was 90% at 10–15% conversion in isomerization of PO over Fe-MCM-41 in toluene at room temperature for 10 min. However, the selectivity towards CA was 67–70% at 42–70% conversion. Amount of Fe in Fe-MCM-41 was 8.4–8.9 wt%. Similar result was demonstrated in isomerization of PO in dichloroethane over Fe-MCM-41 containing iron 3.5–4.1 wt% [15]. Unfortunately, in both cases effect of iron content on activity and selectivity of the reaction was not investigated. Note that iron-containing microporous and mesoporous materials have been mainly investigated as catalysts of oxidation, whereas study about their application in isomerization of PO was rarely reported.

In this work, we examined the role of iron content in the catalytic performance of new Fe-containing materials, such as Fe-containing mesoporous mesophase silica materials (Fe-MMM-2) and microporous Fe-containing nickel phosphate molecular sieves (Fe-VSB-5). According to Refs. [16,17], the structure of VSB-5 and Fe-VSB-5 is based on octahedral NiO₆ units linked by a tetrahedral HPO₄ and PO₄, forming one-dimensional 24-membered ring channel structures with unit cell formula of Ni₂₀[OH]₁₂((H₂O)₆)[(HPO₄)₈(PO₄)₄]·12H₂O. Gao et al. [18] analyzed acidic properties of VSB-5 by method of desorption temperature of ammonia (NH₃-TPD) and found that VSB-5 possessed 263 μmol/g of weak acid sites (a peak at 200 °C). The

existence of LAS formed by Ni ions in VSB-5 was proved by IR spectroscopy using benzonitrile (PhCN) as a probe molecule. Note that the insertion of iron ions into the VSB-5 framework leads to the appearance of new LAS formed by Fe ions. At the same time Fe-MMM-2 has an ordered hexagonal arrangement of uniform mesopores with a diameter of 3.75–3.85 nm and silicate wall thickness 1.3–1.4 nm [19]. According to the comparative analysis of nitrogen adsorption, Fe-MMM-2 has no micropores and possesses high internal and low external surface areas. Moreover, these materials possess acid sites [20] which can favour the high selectivity towards CA. We can suggest that Fe-VSB-5 and Fe-MMM-2 materials, like zeolites, possess high surface areas, unique well-defined pore openings and surface acidity and therefore, have potential in this reaction. Therefore, in this work, we examined the role of textural and acid properties in the catalytic performance of these materials in the rearrangement of PO to CA.

2. Experimental

2.1. Materials

α -Pinene oxide (98.0%) was purchased from Acros Organics. Octane, FeCl₂·4H₂O, NiCl₂·6H₂O, FeCl₃·6H₂O and Na₂SiO₃ were purchased from Merck.

2.2. Synthesis of catalysts

VSB-5 and Fe-VSB-5 materials were hydrothermally synthesized at pH = 7.3 with microwave irradiation according to a reported procedure in Refs. [16,17]. H₃PO₄, FeCl₂·4H₂O and NiCl₂·6H₂O were used as the sources of phosphorous, iron and nickel, respectively. The designation of the samples, the reaction conditions of synthesis, chemical composition and textural data of VSB-5 and Fe-VSB-5 samples are shown in Table 1 and Supporting Information.

Fe-MMM-2 were synthesized hydrothermally according to the procedure which generally included mixing of three solutions (0.2 M aqueous solution of cetyltrimethylammonium bromide (CTAB) (pH 1.0, HCl); 0.5 M FeCl₃ and 0.12 M aqueous solution of a silica sol (pH 1.0, HCl)) [16,17]. Na₂Si₂O₅ and FeCl₃·6H₂O were used as the sources of silicon and iron, respectively. All three solutions were clear and transparent. The solutions were mixed and the final pH was adjusted to 2.0 using 4 M HCl. The synthetic mixtures were kept overnight under ambient conditions and then hydrothermally treated at 50 °C for 24 h. The resulting precipitate was filtered off, washed with distilled water, dried in air at 120 °C for 24 h, and calcined at 600 °C for 5 h. Chemical composition and textural data of Fe-MMM-2 samples are shown in Table 2 and Supporting Information.

2.3. Instrumental measurements

The porous structure of the materials was determined from the adsorption isotherm of N₂ at –196 °C on a Micromeritics ASAP 2400 equipment. The specific surface area (S_{BET}) was calculated from adsorption data over the relative pressure range between 0.05 and 0.20. The total pore volume (V_{total}) was calculated from the amount of nitrogen adsorbed at a relative pressure of 0.99. The X-ray diffraction patterns were measured on an X-ray diffractometer (ThermoARL) with Cu-K_α (λ = 1.5418 Å) radiation. The chemical analyses were done by means of an inductively coupled plasma-atomic emission spectrometry (ICP-AES).

To study Brønsted and Lewis surface acidity by pyridine adsorption, samples were pretreated within the IR cell. Fe-VSB-5 samples were pretreated by heating for 1 h in air and for 1 h under vacuum at 200 °C, while Fe-MMM-2 samples were pretreated by heating for 1 h in air and for 1 h under vacuum at 450 °C. The

Table 1

The reaction conditions of synthesis, chemical composition and textural data of VSB-5 and Fe-VSB-5 samples.

	Preparation gel (atomic %)		Chemical composition			Textural data ^b				
	x^a	$\frac{\text{Fe}}{\text{Fe}+\text{Ni}+\text{P}}$	Weight content (wt%)			Atomic ratio (%)	$\frac{\text{Fe}}{\text{Fe}+\text{Ni}+\text{P}}$	S_{BET} (m^2/g)	V_{Σ} (cm^3/g)	V_{μ} (cm^3/g)
			Fe	Ni	P					
VSB-5	0	0	0	48.5	12.8	0		284	0.24	0.13
3.1%Fe-VSB-5	0.09	5	3.1	43.5	12.8	4.58		202	0.13	0.08
6.5%Fe-VSB-5	0.18	10	6.5	39.8	12.0	9.92		203	0.16	0.09

^a Molar composition of reaction mixture is $x\text{FeCl}_2\text{:}0.63\text{H}_3\text{PO}_4\text{:}1.0\text{NiCl}_2\text{:}3.0\text{NH}_3\text{:}100\text{H}_2\text{O}$.

^b S_{BET} —specific surface area; V_{Σ} —total pore volume; V_{μ} —micropore volume.

Table 2

Textural data and chemical composition of Fe-MMM-2.

	Fe (wt%)	S_{BET} (m^2/g)	V_{meso} (cm^3/g)	S_{ext} (m^2/g)	D (nm)	d_{10} (nm)	w (nm)
Si-MMM-2	0	981	0.45	20	3.0	3.75	1.3
1.0% Fe-MMM-2	1.0	962	0.44	25	3.0	3.85	1.4
1.7% Fe-MMM-2	1.7	970	0.45	36	3.0	3.84	1.4
3.9% Fe-MMM-2	3.9	995	0.45	34	3.0	3.84	1.4
5.9% Fe-MMM-2	5.9	942	0.43	35	3.0	3.85	1.4

S_{BET} —specific surface area; V_{meso} —mesopore volume; S_{ext} —external surface area of mesopore; d_{10} —mesopore interlayer spacing; D —diameter of pore; w —pore wall thickness.

$$D = 2/\sqrt{3}d_{10} \left(V_{\text{meso}}/1/\rho + V_{\text{meso}} \right)^{\frac{1}{2}}, \quad w = 2/\sqrt{3}d_{10} - D.$$

samples were exposed to saturated pyridine vapours at room temperature for 10 min and were heated at 150 °C for 15 min. Then pyridine was desorbed for 30 min under vacuum at 150 °C. The strength of BAS of materials was characterized by the proton affinity values (PA) according to Ref. [21]. The amount of BAS and LAS was estimated from the intensity of the band of the stretching vibration of pyridinium ions with a maximum at 1540 cm⁻¹ (BAS) and 1450 cm⁻¹ (LAS) and using extinction coefficients of $\varepsilon_{\text{LAS}} = 1.67 \pm 0.1$ and $\varepsilon_{\text{BAS}} = 2.22 \pm 0.1 \text{ cm}/\mu\text{mol}$ [22]. The strength of BAS of samples was characterized by the proton affinity values (PA) [23]. For the analysis of the Lewis surface acidity by PhCN adsorption the VSB-5 and Fe-VSB-5 samples were exposed to saturated PhCN vapours at room temperature. FT-IR spectra of the adsorbed PhCN were recorded every 10 min up to saturation by PhCN. FT-IR spectra were recorded on a Shimadzu FTIR-8300S spectrometer in the range of 400–6000 cm⁻¹ with a resolution of 4 cm⁻¹.

2.4. Catalytic test

The isomerization of PO was carried out at 30 °C in a glass reactor equipped with magnetic stirrer. Dichloroethane was used as a solvent. Before reaction all catalysts were activated at 150 °C for 4 h in order to remove adsorbed water. Then 25 or 75 mmol of PO, 2 ml of dichloroethane, 10 mmol of octane (internal standard) and 5 mg of catalyst were added into reactor. At different time intervals aliquots were taken from reaction mixture and analyzed. A mass-spectrometer (Shimadzu GCMS QP-2010 Ultra with column

GsBP1-MS 30 m × 0.32 mm, thickness 0.25 μm) was used for identifying the reaction products. A gas chromatograph (Agilent 7820) with a flame ionization detector on capillary column HP-5 was used to analyze products quantitatively.

3. Results and discussion

Here, we investigated effect of Fe content on the nature of acid sites and catalytic performance of Fe-VSB-5 and Fe-MMM-2, because variation of iron state in Fe-containing materials can change amount of LAS, the dispersion of the Fe-active phase, and accessibility of Fe ions for adsorption of reactants. The main attention was focused on distribution of products in isomerization of PO, which strongly depends on nature of acid sites. We also tried to reveal effect of textural properties of Fe-containing materials on activity and selectivity of this reaction.

3.1. Catalytic performance of Fe-VSB-5 materials

VSB-5 and Fe-VSB-5 were prepared in weakly basic conditions at pH 7.5. The textural data of VSB-5 and Fe-VSB-5 materials are shown in Table 1. These data point that Fe-VSB-5 are microporous materials with high specific area. The crystallinity, morphology and textural properties do not change substantially after the incorporation of iron into framework (Table 1 and Fig. S1 (Supporting information)).

Table 3

Isomerization of PO over Fe-containing materials ^a.

Run		PO conversion (%)	Selectivity (%mol)			
			(CA)	(trans-Carv)	(trans-Sobr)	Other
1	VSB-5	89	55	11	5	29
2	3.1%Fe-VSB-5	92	62	14	5	19
3	6.5%Fe-VSB-5	95(96) ^b	67(64) ^b	16(15) ^b	5(7) ^b	12(14) ^b
4	Si-MMM-2	15	14	61	11	14
5	1.0%Fe-MMM-2	97	58	16	5	21
6	1.7%Fe-MMM-2	93(95) ^b	53(55) ^b	14(15) ^b	5(6) ^b	28(24) ^b
7	3.9%Fe-MMM-2	92	51	16	5	28
8	5.9%Fe-MMM-2	97	46	14	5	34

^a Experimental condition: 0.25 mmol PO in 2 ml dichloroethane, 5 mg catalyst, 30 °C, 30 min.

^b Catalyst was filtered off after 30 min of reaction and the filtrate was stirred at 30 °C for 30 min.

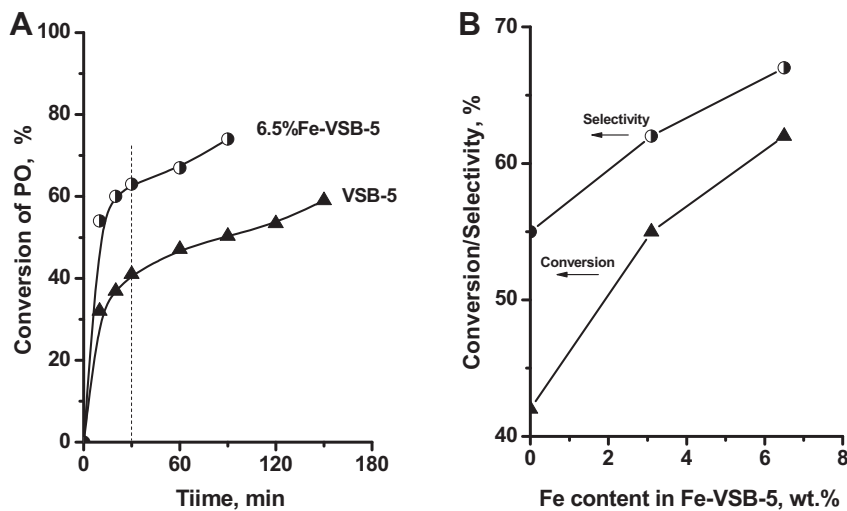


Fig. 1. (A) Kinetic curves of isomerization of PO over VSB-5 and 6.5%Fe-VSB-5 (reaction conditions: 0.75 mmol PO in 2 ml dichloroethane, 5 mg catalyst, 30 °C); (B) effect of iron content in Fe-VSB-5 on conversion of PO and selectivity towards CA (reaction time was 30 min).

The results of the catalytic performance of VSB-5 and Fe-VSB-5 samples are presented in Table 3. Kinetic curves are shown in Fig. 1A. Experimental data clearly show that VSB-5 proved to be very active in isomerization of PO at 30 °C in dichloroethane. CA was the main product with 55% selectivity at 89% conversion of 0.25 mmol PO for 30 min. Moreover, *trans*-carv and *trans*-sobr were also detected in amount around 11% and 5%, respectively. The obtained results indicate that VSB-5 possesses both LAS and BAS (Scheme 1). After the insertion of Fe into VSB-5 network, conversion of PO and the isomer selectivity towards CA increase to 95% and 67%, respectively. Reaction did not proceed after separation of catalyst that was confirmed in special experiments. A 6.5%Fe-VSB-5 sample was filtered off after 30 min of reaction in dichloroethane at 30 °C, and then the filtrate was stirred at 30 °C for 30 min (Table 3, run 3). No conversion of PO was observed after catalyst removing, providing evidence of heterogeneous catalysis.

As one can see from the experimental evidence (Fig. 1B), the catalytic activity of Fe-VSB-5 samples and the isomer selectivity with regard to CA can be adjusted by the Fe content. The larger amount of iron in Fe-VSB-5, the higher yield of CA. We can assume that this result is related with the change of nature of acid sites. Noteworthy, no iron oligomeric species were observed in Fe-VSB-5 samples with 1–6.5 wt% iron content (Fig. S3 (Supporting information)) [24].

Early it has been shown [24] that PhCN can be used for analysis of LAS of VSB-5 and Fe-VSB-5. Band at 2282 cm⁻¹ observed in a spectrum of PhCN adsorbed on VSB-5 can be assigned to the interaction between the nonbonding electrons of PhCN and electron-deficient Ni ions (LAS) (Fig. 2A). At the same time in a spectrum of 6.5%Fe-VSB-5 we can reveal two bands at 2282 cm⁻¹ and 2268 cm⁻¹ (Fig. 2A). A new band can be attributed to the interaction between the nonbonding electrons of PhCN and the electron-deficient Fe ions. We estimated the integral intensities (S_{d}) of bands at 2282 cm⁻¹ and 2268 cm⁻¹. The results show that the increasing iron contents in Fe-VSB-5 leads to an increase in integral intensity of band at 2268 cm⁻¹, which can be considered as an indicator of the increase in the amount of LAS formed by Fe ions (Fig. 2B). At the same time integral intensity of band at 2282 cm⁻¹ decreases with increasing of Fe content in Fe-VSB-5 that can point to the decrease in the amount of LAS formed by Ni ions. Therefore, according to experimental evidence isomorphous substitution of a nickel ion by iron ions leads to the change in nature of LAS. The larger amount of Fe ions, the lower amount of LAS formed by Ni ions and larger amount of LAS formed by Fe ions.

It is well-known that LAS favour formation of CA [3]. It is reasonable to suggest that catalytic properties of Fe-VSB-5 are determined by Lewis acidity (Fig. 1B and 2B), because selectivity towards CA and

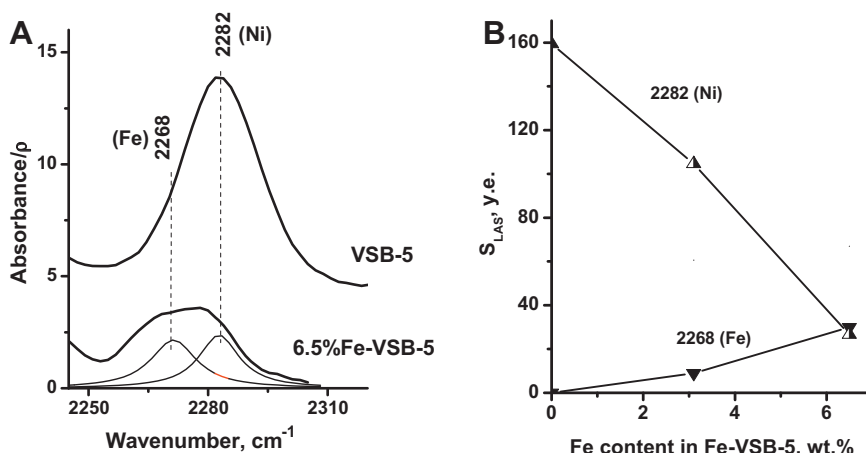


Fig. 2. (A) IR spectra of PhCN adsorbed on VSB-5 and 6.5%Fe-VSB-5; and (B) correlation between iron content in Fe-VSB-5 and integral intensities of bands at 2268 cm⁻¹ and 2282 cm⁻¹.

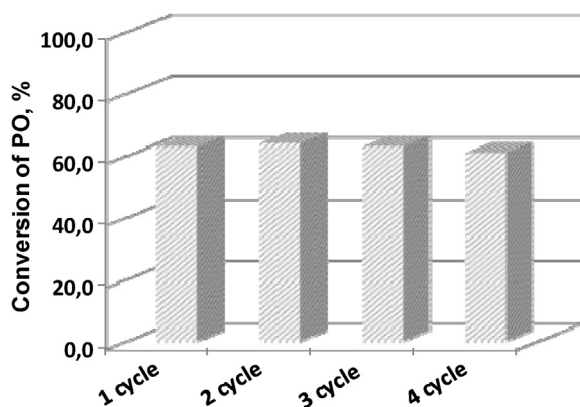


Fig. 3. 6.5%Fe-VSB-5 recycling in isomerization of PO (amount of reactants was corrected based on reaction conditions: 0.75 mmol PO in 2 ml dichloroethane, 5 mg catalyst, 30 °C, 30 min).

integral intensities (S_q) of the band at 2268 cm⁻¹ rise with increasing of Fe content in Fe-VSB-5. Note that we do not exclude the effect of Ni active sites on activity and selectivity. However, the insertion of Fe into VSB-5 framework stronger affects selectivity towards CA in comparison with Ni ions.

The larger amount of LAS in 6.5%Fe-VSB-5 in comparison with VSB-5 was also confirmed by IR spectroscopy using pyridine as probe molecules (Table 4). BAS were also identified in samples. The amount of BAS is about 1 μmol/g that is nearly twice less than LAS in VSB-5. At the same time 6.5%Fe-VSB-5 possesses about 6 μmol/g of BAS that is nearly two times less than that of LAS. We can assume that the acid sites arise from the equilibrium between bridging OH-groups, paired centres of Lewis sites and P-OH groups. Probably, the increasing of LAS amount arises from the different atomic radius of Ni(II) and Fe(II-III) that can lead to the appearance of defect electron-deficient sites (LAS). The difference in amount of BAS between VSB-5 and Fe-VSB-5 materials affects difference in selectivities towards *trans*-carv (Tables 3 and 4). The low selectivity towards *trans*-carv (11%) in the presence of VSB-5 is related to the low amount of BAS.

Importantly, 6.5%Fe-VSB-5 can be used repeatedly without significant loss of catalytic activity during at least four catalytic cycles (Fig. 3). The used 6.5%Fe-VSB-5 can be separated from the reaction mixture by simple filtration, washed by dichloroethane, dried in air and activated at 150 °C for 4 h.

3.2. Catalytic performance of Fe-MMM-2 materials

Fe-MMM-2 samples were prepared in acidic conditions at pH 2.0. The textural data of samples are shown in Table 2, Figs. S3 and S5 (Supporting information). As one can see from the data shown

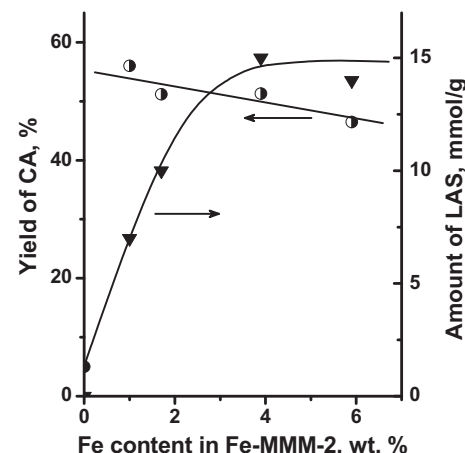


Fig. 4. (A) Effect of iron content in Fe-MMM-2 on yield of CA and amount of LAS (yield of CA was determined by GLH); (reaction conditions: 0.25 mmol PO in 2 ml dichloroethane, 5 mg catalyst, 30 °C, 30 min).

■ Conversion of PO, %
▨ Selectivity towards CA, %
▨ Selectivity towards *trans*-carveol, %

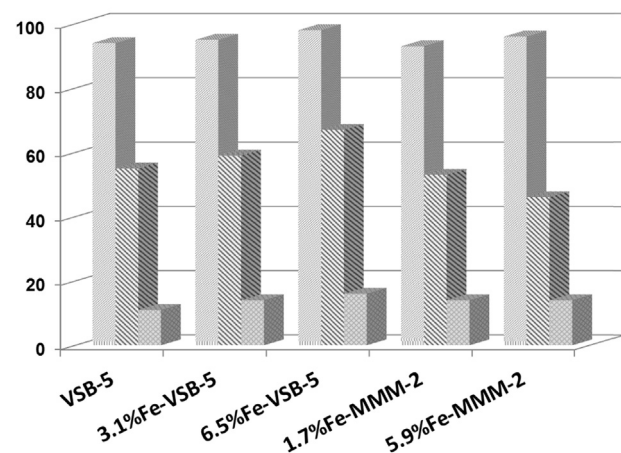


Fig. 5. Isomerization of PO over Fe-containing materials (reaction condition: 0.25 mmol PO in 2 ml dichloroethane, 5 mg catalyst, 30 °C, 30 min).

in Table 2, the wall thickness of Fe-MMM-2 synthesized at pH 2.0 is slightly higher (1.4 nm) compared to the pure siliceous MMM-2 (1.3 nm). This can be explained by the incorporation of larger Fe ions into the silica framework of MMM-2 to replace smaller ions Si⁴⁺. The synthesized Fe-MMM-2 materials have relatively thick

Table 4

Brunsted and Lewis acidity of Fe-VSB-5 and Fe-MMM-2 materials determined by FTIR spectroscopy using pyridine as a probe molecule.

Run		Brunsted acid sites		N_{LAS}/N_{BAS} (mol/mol)
		N_{BAS}^a (μmol/g)	PA ^b (kJ/mol)	
1	VSB-5	1.0	1213	1.8
2	3.1%Fe-VSB-5	3.2	1180	1.9
3	6.5%Fe-VSB-5	6.0	1152	2.1
4	Si-MMM-2	n.d.	1390 ^c	-
5	1% Fe-MMM-2	0.5	1185	11.4
6	1.7% Fe-MMM-2	2.8	1175	3.7
7	3.9% Fe-MMM-2	6.2	1180	2.8
8	5.9% Fe-MMM-2	5.9	1188	2.5

^a N_{BAS} and N_{LAS} —amount of BAS and LAS, correspondingly.

^b PA—the proton affinity.

^c 1390 kJ/mol corresponds to the PA of surface OH-groups of Si-MMM-2 (IR spectroscopy using CO as probe molecule) [23].

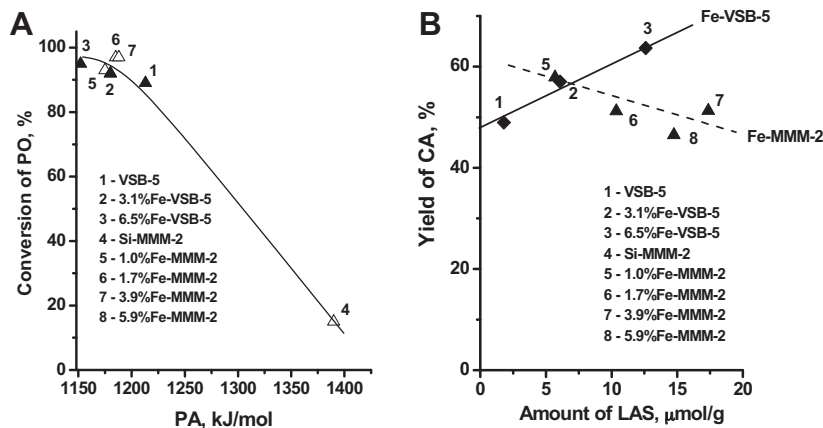


Fig. 6. (A) Correlation between conversion of PO and strength of BAS for Fe-MMM-2 and Fe-VSB-5, (B) Correlation between yield of CA and amount of LAS for Fe-MMM-2 and Fe-VSB-5 (reaction condition: 0.25 mmol PO in 2 ml dichloroethane, 5 mg catalyst, 30 °C, 30 min).

Table 5

Isomerization of PO over Fe-containing mesoporous silica materials.

	Conversion of PO, (%)	Selectivity of CA (%mol)	TON ^c (mol/mol)
1.7%Fe-MMM-2 ^a	78	56	385
3.9%Fe-MMM-2 ^a	84	52	190
4.1%Fe-MCM-41 ^b [15]	70	70	29

^a Experimental condition: 0.75 mmol PO in 2 ml dichloroethane, 5 mg catalyst, 30 °C, 30 min.

^b 0.75 mmol PO in 5 ml dichloroethane, 25 mg catalyst, 40 °C, 3 h.

^c TON = ΔPO/Fe.

walls, which is one of the factors responsible for their hydrothermal stability.

Catalytic properties of iron-containing mesoporous silica materials (Fe-MMM-2) are somewhat different from that of Fe-VSB-5. The main results of catalytic tests of Fe-MMM-2 samples are presented in Table 3. Similar to the reactions with Fe-VSB-5 catalyst, reaction did not proceed either after removing Fe-MMM-2 catalyst (Table 3, run 6). The main product, with Fe-MMM-2, was CA with selectivity around 46–58%.

The iron content in Fe-MMM-2 also affects the reaction rate and distribution of product (Table 3 and Fig. 4). Note that reaction proceeds in the presence of Si-MMM-2. Conversion of PO is 15% for 30 min (Table 3, run 4). However *trans*-carv is the main product with selectivity of 61% that is likely related with the acidic medium of synthesis (pH 2.0). The increase in iron content in Fe-MMM-2 leads to the decrease in selectivity towards CA. This phenomenon cannot be explained by the change in amount of LAS, because according to IR spectroscopy using pyridine as a probe molecule (Table 4), amount of LAS increases with increasing of iron content in Fe-MMM-2. We can assume that this phenomenon is related to change in agglomeration of iron species in an Fe-MMM-2 structure. In our earlier work [19], we demonstrated that the agglomeration of iron and formation of oligomerized iron species was observed in Fe-MMM-2 when Fe content was more than 3.7 wt% (Fig. S4 (Supporting information)).

Of particular interest was a comparison of the catalytic activities of Fe-containing mesoporous silica materials, i.e. activities of Fe-MMM-2 prepared under acidic conditions (pH 2.0) and Fe-MCM-41 prepared under basic conditions (pH ~11) [15]. As one can see from Table 5, activity of 4.1%Fe-MCM-41 is lower in comparison with 3.9%Fe-MMM-2. Conversion of PO over 4.1%Fe-MCM-41 was 70% at 40 °C for 3 h, while conversion of PO over 3.9%Fe-MMM-2 was 84% at 30 °C for 30 min. At the same time, selectivity towards CA in the presence of 4.1%Fe-MCM-41 (70%) is higher than that in the presence of 3.9%Fe-MMM-2 (56%). This phenomenon can be explained

by the difference in surface acid properties. We can assume that because of the basic conditions of synthesis, 4.1%Fe-MCM-41 has lower amount of BAS in comparison with 3.9%Fe-MMM-2. The low amount of BAS leads to the increase in selectivity towards CA.

3.3. Comparison of catalytic properties

A comparison of the catalytic properties of the Fe-containing zeotype materials is presented in Fig. 5. All tested materials showed high activity and selectivity towards CA. In the presence of all samples conversion of PO is about 89–96% (Table 3). As one can see from Fig. 6A strength of BAS affects the conversion of PO, i.e. activity of samples. The higher the strength of BAS, the higher the reaction rate. Fig. 6B demonstrates correlation between amount of LAS and yield of CA. The yield of CA increases with increasing iron content of microporous Fe-VSB-5 catalysts with the pore diameter of 11 Å [25]. At the same time in the presence of mesoporous Fe-MMM-2 catalysts with the pore diameter of 30 Å yield of CA decreases with increasing of iron content in Fe-MMM-2. Note that yield of CA in the presence of Fe-VSB-5 is larger than that in the presence of Fe-MMM-2. The difference in yields of CA between microporous Fe-VSB-5 and mesoporous Fe-MMM-2 materials is difficult to explain by only difference in amount of LAS and BAS (Table 4). Thus, amount of LAS and BAS is the same in 6.5%Fe-VSB-5 and 5.9%Fe-MMM-2, while selectivity towards CA in the presence of 5.9%Fe-MMM-2 is lower (46%) in comparison with 6.5%Fe-VSB-5 (67%). We can assume that this difference is related to the difference of pore diameters. The unique structure of Fe-VSB-5 with the pore diameter of 11 Å [25] comparable with size of reactants and intermediates may affect the improved selectivity towards CA by a shape-selectivity.

4. Conclusions

Catalytic properties of Fe-containing mesoporous Fe-MMM-2 materials and microporous nickel phosphate molecular sieves Fe-VSB-5 were studied in isomerization of PO. It was demonstrated that these materials favour the rearrangement of PO to CA with 50–67% selectivity in dichloroethane under mild conditions.

Reaction rate and selectivity towards CA over Fe-containing microporous Fe-VSB-5 and mesoporous Fe-MMM-2 materials depend on iron content, which affects the oligomeric state of Fe and amount of LAS. The high yield of CA is attributed to the presence of isolated iron sites in matrix of Fe-VSB-5 and Fe-MMM-2. The yield of CA rises with increasing of iron content in Fe-VSB-5 due to the increase in amount of LAS. However, on the contrary, in spite of increasing of amount of LAS the yield of CA decreases with

increasing of iron content in Fe-MMM-2 that is related to the formation of oligomeric iron oxides species. The higher yield of CA in the presence of Fe-VSB-5, in comparison to Fe-MMM-2, is proposed to be due to transition-state shape selectivity induced by structure of VSB-5.

Acknowledgements

This work was supported by SB RAS project V.44.2.12, the Federal Program "Scientific and Educational Cadres of Russia" (No. 2012-1.5-12-000-1013-002) and Basic Science Research Program through the National Research Foundation of Korea (NRF) funded by the Ministry of Education (Grant No. 2012004528).

References

- [1] C.B. Darr, M.E. Davis, *Catal. Today* 19 (1994) 151–186.
- [2] A. Corma, H. Garcia, *Chem. Rev.* 103 (2003) 4307–4365.
- [3] J. Kaminska, M.A. Schwegler, A.J. Hoefnagel, H. van Bekkum, *Recl. Trav. Chim. Pays-Bas.* 111 (1992) 432–437.
- [4] H. van Bekkum, H.W. Kuowenhoven, *Stud. Surf. Sci. Catal.* 157 (2005) 311–336.
- [5] P.-S. E. Dai, *Catal. Today* 26 (1995) 3–11.
- [6] L. Kurfirtova, Y.-K. Seo, Y.K. Hwang, J.-S. Chang, J. Cejka, *Catal. Today* 179 (2012) 85–90.
- [7] D.B. Ravindra, Y.T. Nie, S. Jaenicke, G.K. Chuah, *Catal. Today* 96 (2004) 147–153.
- [8] P.J. Kunkeler, J.C. van der Waal, J. Bremmer, B.J. Zuurdeeg, R.S. Downing, H. van Bekkum, *Catal. Lett.* 53 (1998) 135–138.
- [9] B. Jarry, F. Launay, J.P. Nogier, J.L. Bonardet, *Stud. Surf. Sci. Catal.* 165 (2007) 791–794.
- [10] W.F. Holderich, J. Roseler, G. Heitmann, A.T. Liebens, *Catal. Today* 37 (1997) 353–366.
- [11] J.B. Lewis, G.W. Hedrick, *J. Org. Chem.* 30 (1965) 4271–4275.
- [12] A. Dhakshinamoorthy, M. Opanasenko, J. Cejka, H. Garcia, *Adv. Synth. Catal.* 355 (2013) 247–268.
- [13] A.T. Liebens, C. Mahaim, W.F. Holderich, *Stud. Surf. Sci. Catal.* 108 (1997) 587–594.
- [14] N.A. Fellenz, J.F. Bengoa, S.G. Marchetti, A. Gervasini, *Appl. Catal. A* 435–436 (2012) 187–196.
- [15] J.V. Coelho, A.L.P. de Meireles, K.A. da S. Rocha, M.C. Pereirac, L.C.A. Oliveira, E.V. Gusevskay, *Appl. Catal. A* 443–444 (2012) 125–132.
- [16] S.H. Jhung, J.W. Yoon, J.-S. Hwang, A.K. Cheetham, J.-S. Chang, *Chem. Mater.* 17 (2005) 4455–4460.
- [17] S.H. Jhung, J.-S. Chang, Y.K. Hwang, J.-M. Greneche, G. Ferey, A.K. Cheetham, J. Phys. Chem. B 109 (2005) 845–850.
- [18] D. Gao, G. Gao, *Catal. Commun.* 8 (2007) 681–685.
- [19] M.N. Timofeeva, M.S. Mel'gunov, O.A. Kholdeeva, M.E. Malyshev, A.N. Shmakov, V.B. Fenelonov, *Appl. Catal. B* 75 (3–4) (2007) 290–297.
- [20] M.N. Timofeeva, M.E. Malyshev, V.N. Panchenko, A.N. Shmakov, A.G. Potapov, M.S. Mel'gunov, *Appl. Catal. B* 95 (2010) 110–119.
- [21] A.A. Davydov, *Molecular spectroscopy of oxide catalyst surfaces*, John Wiley, England, 2003, pp. 1–668.
- [22] G. Kosova, *Stud. Surf. Sci. Catal.* 158 (1998) 59–66.
- [23] E.A. Paukshtis, *Infrakrasnaya Spektroskopiya v Geterogennom Kislotno-Osnovnom Katalize* (Infrared Spectroscopy in Heterogeneous Acid–Base Catalysis), Nauka, Novosibirsk, 1992.
- [24] M.N. Timofeeva, A.Yu. Z. Hasan, V.N. Orlov, Yu. Panchenko, A. Chesarov, I.P. Soshnikov, S.H. Jhung, *Appl. Catal. B* 107 (1–2) (2011) 197–204.
- [25] N. Guillou, Q. Gao, P. Forester, J.-S. Chang, M. Nogues, S.-E. Park, G. Ferey, A.K. Cheetham, *Angew. Chem. Int. Ed.* 40 (2001) 2831–2834.